Andreas Jess[1]
Christoph Kern[1]

[1] Department of Chemical Engineering, University Bayreuth, Bayreuth, Germany.

Research Article

Modeling of Multi-Tubular Reactors for Fischer-Tropsch Synthesis

The results of the simulation of multi-tubular Fischer-Tropsch reactors based on a two-dimensional pseudo-homogeneous model are presented. The model takes into account the intrinsic kinetics of two commercial iron and cobalt catalysts, intraparticle mass transfer limitations, and the radial heat transfer within the fixed bed and to the cooling medium (boiling water). The effective rate with Co is slightly higher than with Fe. Hence, a temperature level can be used for Co that is 20 °C lower compared to Fe. The conversion and product selectivies are then almost the same and the reactor can be operated safely without a temperature runaway. The results of the simulations are consistent with literature data and show that there is still room for improvement of fixed bed FT reactors, e.g., by an enhanced heat transfer.

Keywords: Cobalt catalyst, Fischer-Tropsch Synthesis, Fixed bed reactor, Iron catalyst, Reactor modeling

Received: March 12, 2009; *revised:* April 8, 2009; *accepted:* April 14, 2009

DOI: 10.1002/ceat.200900131

1 Introduction

1.1 Background

Production of synthetic fuels via Fischer-Tropsch (FT) synthesis has the potential to produce fuels like gasoline and diesel oil, as well as petrochemicals from fossil and renewable sources. In recent years, the availability of cheap natural gas and solid raw materials, like coal and biomass, has given momentum to FT technology. Thus, the worldwide FT plant capacities will increase significantly in the future; today with natural gas favored as feedstock. Around 2015, the worldwide annual production rate of liquid fuels via FT will be around 30 million tonnes of fuels and chemicals, mostly produced in countries like South Africa, Malaysia, and Qatar.

The FT synthesis can be regarded as a surface polymerization reaction since monomer units are formed from the reagents, hydrogen and carbon monoxide, in situ on the surface of the catalyst, which is usually based on iron or cobalt. Hence, a variety of hydrocarbons (mainly paraffines) are formed by successive addition of C_1 units to growing chains on the surface of the catalyst. This main reaction of the FT synthesis is represented by:[1)]

$$CO + 2\,H_2 \rightarrow (-CH_2-) + H_2O \qquad \Delta_R H^0_{298} = -152\ \text{kJ mol}^{-1} \quad (1)$$

whereby the term, $(-CH_2-)$, represents a methylene group of a normal paraffin. For a kinetic description of the synthesis, methane formation is often considered as a separate reaction:

$$CO + 3\,H_2 \rightarrow CH_4 + H_2O \qquad \Delta_R H^0_{298} = -206\ \text{kJ mol}^{-1} \quad (2)$$

The third reaction that plays an important role – at least if iron-based catalysts are used – is the unwanted formation of carbon dioxide by the water-gas shift reaction.

$$CO + H_2O \rightarrow CO_2 + H_2 \qquad \Delta_R H^0_{298} = -41\ \text{kJ mol}^{-1} \quad (3)$$

Two reactor types are currently favored for FT; at least, for low-temperature synthesis ($T < 250$ °C), the multi-tubular fixed bed and the slurry bubble column reactor. One main advantage of the multi-tubular reactor is that a modular scale-up is possible from data from a representative, single tube. Nevertheless, reactor modeling is still needed to optimize the reactor with regard to productivity and safety aspects (temperature runaway). Such modeling has to take into account the intrinsic kinetics, pore diffusion limitations, and the radial heat transfer from the fixed bed to the wall and, finally, to the cooling medium, which is usually boiling water.

1) List of symbols at the end of the paper.

Correspondence: Prof. Dr.-Ing. A. Jess (Jess@uni-bayreuth.de), Department of Chemical Engineering, University Bayreuth, D-95440 Bayreuth, Germany.

1.2 Objectives and Methodology

In contrast to slurry phase FT reactors, the literature on fixed bed reactor modeling and design is very limited. According to a recent summary of the current status given by Steynberg et al. [1], only five serious modeling studies on FT fixed bed reactors have been reported in the (open) literature [2–7]. In a study not mentioned by Steynberg et al. – as it was published just recently – Guettel and Turek also presented a simulation study of FT reactors [8].

Atwood and Benett [2] proposed a one-dimensional, heterogeneous plug flow model to investigate parameter effects on commercial reactors. Bub et al. [3] developed a two-dimensional, pseudo-homogeneous plug flow model, but intraparticle diffusion limitations were neglected. In our previous work, a pseudo-homogeneous two-dimensional model was used, but exclusively for converting nitrogen-rich syngas [4]. Recently, Wang et al. [5] proposed a heterogeneous one-dimensional model to account for pore diffusion limitations. Remarkably, only De Swart [6, 7] studied FT fixed-bed reactors over a cobalt catalyst by a heterogeneous one-dimensional model, although cobalt is commercially relevant for fixed bed FT reactors (Shell Middle Distillate Process). Guettel and Turek [8] compared different reactor types based on a one-dimensional approach (fixed bed, slurry, monolithic reactor, and mircroreactor), including all mass transfer resistances for cobalt as catalyst, showing the potential of new reactor concepts to decrease mass transfer resistances. All these studies have their specific drawbacks, i.e., either pore diffusion or the radial temperature gradient in the fixed bed (1D model) are neglected, and non of these studies included a comparison of both catalysts (Co and Fe).

Standard textbooks on reactor design and modeling, for example the well-known book of Froment and Bischoff [9], only deal with fixed bed reactors in a fundamental way, e.g., by comparison of one- and two-dimensional models but do not make specific reference to FT.

The objective of this paper was the simulation of a multitubular FT reactor, both for iron and cobalt catalysts, which was until now not done to our best knowledge. Thereby, the attempt was made to cover all main aspects, like the intrinsic kinetics, mass transfer limitations, all heat transfer parameters, comparison of the one- with the two-dimensional model, safety aspects, the influence of the recycle of unconverted syngas, and, finally, the inspection of the room for improvement of fixed bed FT reactors by enhanced heat transfer.

2 Intrinsic and Effective Reaction Rate of Fischer-Tropsch Synthesis

Since the discovery of the synthesis in 1923 by Franz Fischer and Hans Tropsch, the kinetics have been studied extensively and the rate of reaction was described either by using power law rate equations, Langmuir-Hinshelwood equations, or equations based on certain mechanistic assumptions. An overview of rate equations for iron catalysts is given by Huff and Satterfield [10], and for cobalt catalysts by Yates and Satterfield [11]. Details on kinetics and reaction mechanisms are discussed in [12–21].

Today, cobalt and iron are considered to be the most attractive FT-catalysts. Iron, which is cheaper, has a considerable water gas shift activity (Eq. (3)), which is a drawback compared to cobalt since CO_2 is an unwanted byproduct and less valuable hydrocarbons are formed.

Activation in syngas atmosphere requires several hours or even days, during which the metal surface is rearranged or reconstructed (for cobalt) or carbided (for iron). In addition, the pores of the catalyst are filled with liquid higher hydrocarbons (wax), which leads to a decrease of the effective reaction rate by pore diffusion for particle diameters of more than about 1 mm.

Although the number of publications on the kinetics of FTS is numerous (some are listed above), the number with quantitative kinetic equations for commercial catalysts is very limited. Those used in this work for iron and for cobalt are described in the next two subsections.

2.1 Reaction Rate on a Commercial Iron Catalyst

The intrinsic rate of H_2-consumption on a typical commercial iron catalyst (ARGE cat.) was measured by Kuntze and Raak [4, 22, 23] by fixed bed lab-scale experiments with small particles (< 0.2 mm; no influence of pore diffusion):

$$r_{\mathrm{m,H_2,FT}} = -\frac{d\dot{n}_{\mathrm{H_2}}}{dm_{\mathrm{cat}}} = k_{\mathrm{m,H_2,HW}} \frac{c_{\mathrm{H_2,g}}}{1 + K_{\mathrm{HW}} \frac{c_{\mathrm{H_2O,g}}}{c_{\mathrm{CO,g}}}} \tag{4}$$

This Hougen-Watson type equation considers the inhibiting influence of H_2O on the rate.

The intrinsic reaction rate constant, $k_{\mathrm{m,H2,HW}}$, and the coefficient, K_{HW}, are:

$$k_{\mathrm{m,H_2,HW}} = 1.2 \cdot 10^7 m^3 kg^{-1} s^{-1} e^{\frac{-109000}{\mathrm{RT}}} \tag{5}$$

$$K_{\mathrm{HW}} = 0.2 e^{\frac{8.800}{\mathrm{RT}}} \tag{6}$$

($1.7 > K_{\mathrm{HW}} > 1.5$ for 220 °C < T < 250 °C)

For particles with diameters used in technical fixed bed reactors (d_p > 1 mm), an effective rate considering pore diffusion has to be used:

$$r_{\mathrm{m,H_2,eff,FT}} = \eta_{\mathrm{pore}} \left(\frac{k_{\mathrm{m,H_2,HW}}}{1 + K_{\mathrm{HW}} \frac{c_{\mathrm{H_2O,g}}}{c_{\mathrm{CO,g}}}} \right) c_{\mathrm{H_2,g}} = \eta_{\mathrm{pore}} k_{\mathrm{m,H_2}} c_{\mathrm{H_2,g}} \tag{7}$$

The term in brackets can be regarded as a pseudo-first order rate constant ($k_{\mathrm{m,H2}}$). The influence of pore diffusion is considered by the effectiveness factor, η_{pore}:

$$\eta_{\mathrm{pore}} = \frac{r_{\mathrm{m,H_2,eff}}}{k_{\mathrm{m}}, \mathrm{H_2} c_{\mathrm{H_2,g}}} = \frac{\tanh \phi}{\phi} \approx \frac{1}{\phi} \tag{8}$$

(for $\phi \geq 2$)

and the Thiele modulus in case of FT synthesis is given by:

$$\phi = \frac{V_{\mathrm{p}}}{A_{\mathrm{p,ext}}} \sqrt{\frac{k_{\mathrm{m,H_2}} \rho_{\mathrm{p}} c_{\mathrm{H_2,g}}}{D_{\mathrm{eff,H_2,l}} c_{\mathrm{H_2,l}}}} \tag{9}$$

$V_p/A_{p,ex}$ is the ratio of particle volume to the external surface area, and $c_{H2,l}$ is the concentration of hydrogen in liquid wax, calculated by the Henry coefficient ($H_{H2,c} \approx 20{,}000$ Pa m^3 mol^{-1}):

$$c_{H_2,l} = \frac{p_{H_2,g}}{H_{H_2,c}} = \frac{RT}{H_{H_2,c}} c_{H_2,g} \tag{10}$$

By combining Eqs. (9) and (10), we get the following equation for the Thiele modulus:

$$\phi = \frac{V_p}{A_{p,ex}} \sqrt{\frac{k_{m,H_2}\rho_p}{D_{eff,H_2,l}\frac{RT}{H_{H_2,c}}}} \tag{11}$$

The effective diffusion of the dissolved hydrogen in the liquid-filled porous catalyst is described by an effective diffusion coefficient, $D_{eff,H2,l}$, which considers that only a portion of the particle is permeable and that the path through the particle is random and tortuous. Both aspects are taken into account by the porosity, ε_P, and the tortuosity, τ_P:

$$D_{eff,H_2,l} = \frac{\varepsilon_p}{\tau_p} D_{mol,H_2,l} \approx 0.3 D_{mol,H_2,l} \tag{12}$$

(for FT on Fe)

The molecular diffusivity of H_2 in liquid FT products is calculated by the Wilke-Chang equation [24]. For temperatures from 200 to 260 °C, $D_{mol,H2,l}$ is about $4 \cdot 10^{-8}$ m^2 s^{-1} [23] and ε_P/τ_P is 0.3 [22, 23].

Fig. 1 (left) shows the effective rate constant of H_2-consumption for a value of $V_p/A_{p,ex}$ of 0.5 mm (cylindrical particles; length: 5 mm, diameter: 2.7 mm). Hence, pore diffusion strongly affects the effective rate constant for temperatures above 180 °C. The reason for this strong influence is the slow diffusion of the dissolved H_2 in the liquid-filled pores of the catalyst.

External diffusion limitations are negligible for temperatures below about 400 °C, which is an unrealistically high temperature for FT synthesis.

Fig 1 (right) indicates that the influence of pore diffusion would only be negligible (at temperatures relevant for FT fixed bed synthesis, 200–250 °C) if $V_p/A_{p,ex}$ is less than 0.03 mm, e.g., for spherical particles with a diameter < 0.18 mm. Hence, for a technical particle size in the range of millimeters and a typical temperature of 240 °C, only about 20 % of the particle is used for FT-synthesis which has to be accepted to limit the pressure loss in fixed bed reactors.

For an accurate modeling of a FT fixed bed reactor, not only the main reaction (Eq. (1), index FT) leading to the formation of higher hydrocarbons, but also methane formation (Eq. (2), index M) and the water gas shift reaction (Eq. (3), index S) must be considered. The rate equations for these three reactions were determined by systematic experiments with the commercial Fe catalyst in its original form (cylinders: 2.7 mm in diameter, 5 mm in length) [25]. The following equations were derived (see also [4]):

$$r_{m,H_2,FT} = -\frac{d\dot{n}_{H_2}}{dm_{cat}} = \frac{k_{m,H_2,eff,FT} c_{H_2,g}}{1 + 1.6\frac{c_{H_2O,g}}{c_{CO,g}}} \tag{13}$$

$$(\text{with } k_{m,H_2,eff,FT} = 5.1 m^3 kg^{-1} s^{-1} e^{\frac{-52000}{RT}})$$

$$r_{m,H_2,M} = -\frac{d\dot{n}_{H_2}}{dm_{cat}} = k_{m,H_2,eff,M} c_{H_2,g} \tag{14}$$

$$(\text{with } k_{m,H_2,eff,M} = 27.3 m^3 kg^{-1} s^{-1} e^{\frac{-70000}{RT}})$$

$$r_{m,H_2,S} = \frac{d\dot{n}_{H_2}}{dm_{cat}} = k_{m,H_2,eff,S} c_{H_2O,g} \tag{15}$$

$$(\text{with } k_{m,H_2,eff,S} = 155 m^3 kg^{-1} s^{-1} e^{\frac{-70000}{RT}})$$

For the conditions of the Fischer-Tropsch reaction (about 250 °C) with a syngas free of CO_2, the reverse reaction of the shift reaction, i.e., the formation of CO and H_2O from H_2 and CO_2 is negligible as the equilibrium is on the side of H_2 and CO_2.

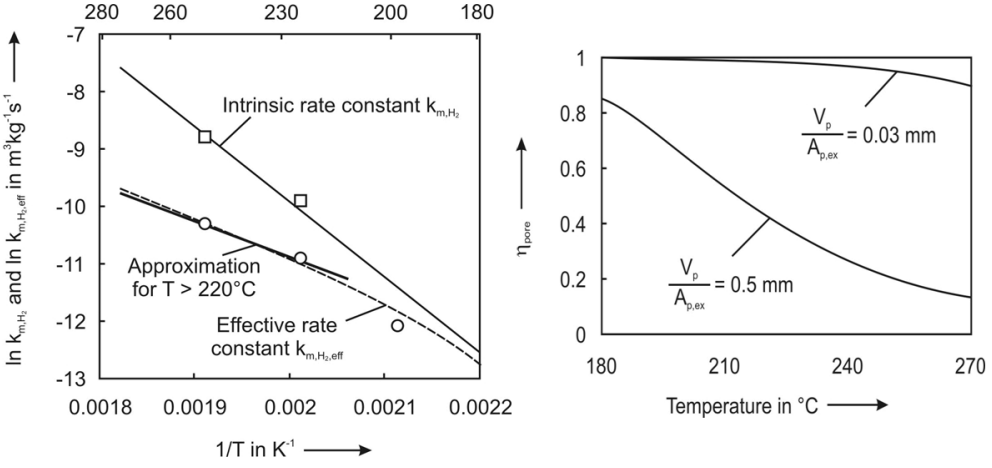

Figure 1. Intrinsic and effective rate constant of H_2-consumption for an iron catalyst. Left: cylinders, 2.7 mm in diameter and 5 mm in length, i.e., $V_p/A_{p,ex} = 0.5$ mm (measured in [23, 25]). Right: values for two particle sizes (calculation was done exemplarily for a syngas free of steam, i.e., for $c_{H2O}/c_{CO} \approx 0$; thus, $k_{m,H2,HW} = k_{m,H2}$ and $k_{m,H2,eff,FT} = \eta_{pore}\, k_{m,H2}$).

The effective rate constant, $k_{m,H2,eff,FT}$, of Eq. (13) is shown in Fig. 1 as the "approximation for $T > 230\,°C$" and shows a very good agreement with the theoretical values based on the Thiele approach (dashed line). The apparent activation energy of 52 kJ/mol (Eq. (13)) is about half of the intrinsic value (109 kJ/mol, Eq. (5)), as expected for a strong limitation by pore diffusion.

Note that Eqs. (13)–(15) are only valid if the influence of pore diffusion is fully developed, i.e., for $T > 220\,°C$ and for a particle diameter of 3 mm ($V_p/A_{p,ex} = 0.5$ mm).

2.2 Reaction Rate on a Commercial Cobalt Catalyst

The intrinsic rate constant of H_2-consumption on a commercial cobalt catalyst was determined by Yates and Satterfield [11], and Maretto and Krishna [26]. According to Steynberg et al. [1], the intrinsic activity of modern industrial Co-catalysts is by a factor of three higher than those reported by these authors. Based on the data given in the abovementioned literature, the equation of hydrogen consumption on a commercial Co-catalyst was estimated (using the threefold values) by:

$$r_{m,H_2} = -\frac{d\dot{n}_{H_2}}{dm_{cat}} = k_{m,H_2,LH} c_{H_2,g} \frac{c_{CO,g}}{\left(1 + K_{CO} c_{CO,g}\right)^2} \tag{16}$$

The rate constant of this Langmuir-Hinshelwood-type equation and the adsorption coefficient, K_{CO}, are:

$$k_{m,H_2,LH} = 0.8 m^6 mol^{-1} kg^{-1} s^{-1} e^{\frac{-37.400}{RT}} \tag{17}$$

$$K_{CO} = 5 \cdot 10^{-9} m^3 mol^{-1} e^{\frac{68.500}{RT}} \tag{18}$$

Based on these equations, a pseudo first-order rate constant can be determined:

$$r_{m,H_2} = k_{m,H_2} c_{H_2,g} \text{ with } k_{m,H_2} = k_{m,H_2,LH} \frac{c_{CO,g}}{\left(1 + K_{CO} c_{CO,g}\right)^2} \tag{19}$$

and the effectiveness factor for pore diffusion can then be calculated by Eqs. (8)–(12) and (16)–(19) analogously to the procedure used before for the iron catalyst.

The comparison of the effective rate constant of H_2-consumption for cobalt and iron is shown in Fig. 2.

For the given conditions (24 bar, a H_2-to-CO ratio of 2), iron is more active below 210 °C, but such a low temperature is not relevant for a technical reactor. Typical temperature regimes of fixed bed reactors are 200 to 230 °C for cobalt and 220 to 250 °C for iron (see Section 5). Hence, the effective reaction rates are then almost equal.

3 Fischer-Tropsch Processes and Reactors

General aspects of the synthesis and of different processes are discussed in [27–35]. For details on different reactor types used for FT synthesis, we refer to [4, 8, 29, 34–39].

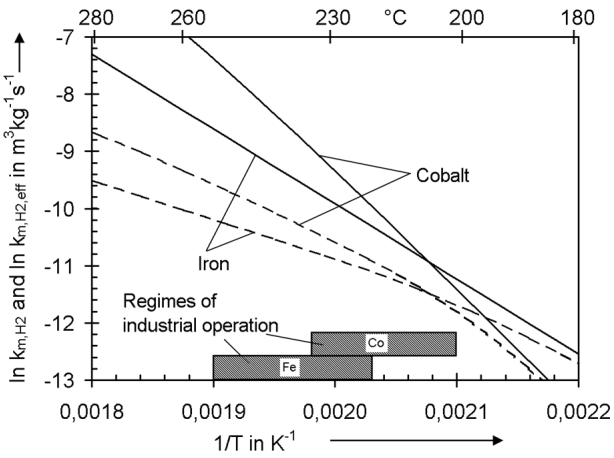

Figure 2. Intrinsic and effective rate constant (depicted as dashed lines) of H_2-consumption on Co and Fe (entrance of reactor, i.e., for Fe, the influence of steam on the rate is still negligible and, for Co, a constant partial pressure of CO of 8 bar was assumed, $V_p/A_{p,ex} = 0.5$ mm).

XTL technology (X to liquids, with X as coal, biomass or natural gas, etc.) based on FT consists of three major parts, syngas generation, FTS, and product upgrading. FTS uses syngas (CO/H_2) generated from coal, biomass or natural gas. The syngas is produced via oxygen/steam gasification (solid fuels) or steam reforming/partial oxidation (natural gas).

For coal and biomass as feedstock, the syngas has to be cleaned of impurities such as H_2S and NH_3, and adjusted to the needs of the subsequent synthesis step. Two temperature ranges are applied, high-temperature (300–350 °C) leading mainly to short-chain alkenes and gasoline, and low-temperature (200–250 °C) mainly leading to wax and diesel oil. In this work, only low-temperature FT fixed bed synthesis is considered.

Upgrading FT products most commonly includes reforming and isomerization to improve the low octane number and hydrocracking of wax to produce more diesel oil.

Among the different products, in particular, diesel oil is highly valuable without upgrading because of its excellent properties. It has a high cetane number of 70 compared to the standard value of 50, and contains near zero sulphur and aromatics.

The most difficult problem to solve in the design of FT reactors is the high exothermicity combined with a high sensitivity of product selectivity to temperature. Hence, an efficient heat removal is needed. Four reactor types are considered today. For low-temperature FT synthesis (< 250 °C), multi-tubular fixed bed and slurry bubble column reactors, and for high-temperature synthesis (T > 300 °C), circulating fluidized bed and bubbling fluid beds (were) are used.

Reactor capacities of modern FT reactors are in the range of up to 900 tonnes of liquid hydrocarbons per day for fixed bed operation (cobalt, 8000 single tubes) and up to 1900 tonnes for a slurry bubble column [40].

Low-temperature reactors have to cope with a three-phase system (gaseous syngas and hydrocarbons, liquid wax, solid

catalyst), whereas high-temperature reactors work in the two-phase regime (syngas, gaseous hydrocarbons, solid catalyst). Heat is transferred via heat transfer surfaces inside the reactor. In a slurry bubble column reactor, small catalyst particles (< 200 μm) are suspended in the part of the product that is liquid at reaction conditions of around 20 bar and 230 °C. The syngas is fed into the bottom of the column. A drawback is the fact that the fine catalyst has to be separated from the liquid products, which is not needed in fixed bed reactors.

Fig. 3 shows a commercial FT fixed bed process, which is in the focus of this work.

The conversion of syngas per pass is about 30 %, but a gas recycle, usually with a recycle ratio of around 2, enables an overall conversion of 90 % (see section 6). The limited conversion per pass helps to remove the reaction heat and a temperature runaway is avoided.

4 Fischer-Tropsch Fixed Bed Reactor Model (Multi-Tubular Reactor)

For the simulation of multi-tubular FT reactors, typical reaction conditions as listed in Tab. 1 were used. One aspect (discussed separately in Section 6) was neglected: The syngas that enters the reactor may not only consist of CO and H_2, but may contain methane and also CO_2, which may be present in the fresh syngas and in the recycle gas.

If dispersion of mass is neglected (which is reasonable as shown by respective calculations), the mass balance for hydrogen yields:

$$-u_s \frac{dc_{H_2}}{dz} = r_{m,H_2}\rho_b \tag{20}$$

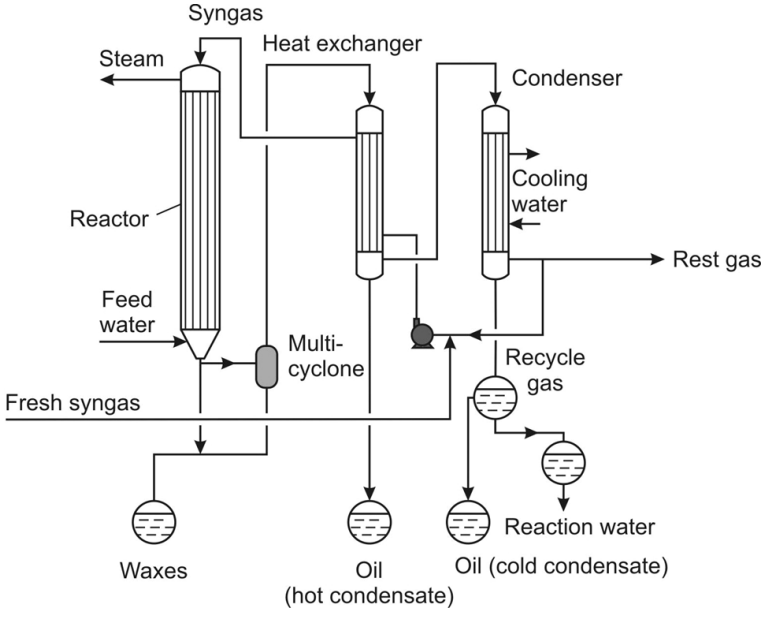

Figure 3. Commercial FT plant (ARGE fixed bed process, adapted from [31]).

The rate of H_2-consumption for an Fe-catalyst (by FT reaction, methane formation, shift) is:

$$r_{m,H_2} = r_{m,H_2,FT} + r_{m,H_2,M} - r_{m,H_2,S} \tag{21}$$

(For cobalt, the shift reaction can be neglected. In this work, methane formation on Co was also not considered as a parallel reaction to the formation of higher hydrocarbons (C_{2+}) because of the lack of reliable data. Thus, only Eq. (16) that represents the overall consumption rate of hydrogen to methane and to C_{2+} was used.)

As inspected in the following, we may model a single tube of the cooled multi-tubular reactor by the so-called one- or two-dimensional fixed bed reactor model.

4.1 Two-Dimensional Fixed Bed Reactor Model

If axial dispersion of heat is neglected, the heat balance of the two-dimensional model is:

$$\rho_{mol} c_p u_s \frac{dT}{dz} = \lambda_{rad}\left(\frac{d^2T}{dr^2} + \frac{dT}{rdr}\right) - \rho_b \sum \Delta_R H_i r_{m,H_2,i} \tag{22}$$

with

$$\sum \Delta_R H_i r_{m,H_2,i} = \Delta_R H_{FT} r_{m,H_2,FT} + \Delta_R H_M r_{m,H_2,M} + \Delta_R H_S r_{m,H_2,S}$$

The boundary conditions are:

$$T = T_{in} \qquad (\text{for } z = 0) \tag{23}$$

$$\frac{dT}{dr} = 0 \qquad (\text{for } r = 0 \text{ and all } z) \tag{24}$$

$$-\lambda_{rad}\frac{dT}{dr} = \alpha_{W,int}\left(T_{W,int,1} - T_{W,int,2}\right) \quad (\text{for } r = 0.5 d_R \text{ at the wall}) \tag{25}$$

The coefficient, $\alpha_{W,int}$, for the heat transfer from the bed to the internal wall was calculated by standard correlations taken from the literature [41, 42]. The coefficient, $\alpha_{W,ex}$, for the external heat transfer from the tube to boiling water was determined by well-known correlations [43], and depends on the vapor pressure and the temperature difference between the tube temperature and the boiling temperature. The coefficient, λ_{rad}, for the radial effective heat conduction in the bed was calculated by correlations given in [41, 44]. The values of all heat transfer parameters are listed in Tab. 1.

Eq. (25) considers the bed and the fluid as a pseudo-homogeneous medium, and the heat transfer within the bed up to the wall is represented by the radial effective thermal conductivity, λ_{rad}, and the internal wall heat transfer coefficient, $\alpha_{w,int}$. Thus, the model assumes a jump in temperature directly at the wall from $T_{W,int,1}$ to $T_{W,int,2}$ (see below in Fig. 7).

Table 1. Data on chemical media and reaction conditions of Fischer-Tropsch synthesis used here to model a multi-tubular fixed bed reactors (all values at 24 bar and 240 °C).

Superficial gas velocity, u_s (empty reactor)[1]	0.55 m s^{-1}
Total molar gas concentration (feed), ρ_{mol}	563 mol m^{-3}
Total pressure, p	24 bar
Diameter of catalyst particle, d_p	3 mm
Length of tubes	12 m
Internal diameter of single tube, $d_{R,int}$[2] (total number of tubes about 2000)	4.6 cm
External diameter of single tube, $d_{R,ex}$	5.6 cm
Bulk density of catalyst bed, ρ_b	Fe-cat.: 790 kg m^{-3} Co-cat.: 700 kg m^{-3}
Inlet concentration of hydrogen	66.6 vol.-% (rest CO)
Kinematic viscosity, ν, of gas mixture (feed)	$4 \cdot 10^{-6}$ $m^2 s^{-1}$
Thermal conductivity of gas mixture (feed), λ_{gas}	0.16 W $m^{-1}K^{-1}$
Effective radial thermal conductivity, λ_{rad}	6.3 W $m^{-1}K^{-1}$
Heat capacity of gas mixture (feed), c_p	30 J $mol^{-1}K^{-1}$
Heat transfer coefficient (bed to internal tube wall), $\alpha_{W,int}$	900 W $m^{-2}K^{-1}$
Thermal conductivity of wall material (steel), λ_{wall}	50 W $m^{-1}K^{-1}$
Heat transfer coefficient (external tube wall to boiling water, 25 bar), $\alpha_{W,ex}$	1600 W $m^{-2}K^{-1}$
Thermal transmittance, U_{wall}	1380 W $m^{-2}K^{-1}$
Overall thermal transmittance, $U_{overall}$	364 W $m^{-2}K^{-1}$

[1]For a CO-conversion of 32 % per pass, and the assumption of a total conversion with recycle of 80 % and a selectivity of 80 % to C_{5+}-hydrocarbons (HCs), the production rate would be 240 t C_{5+} /d for a reactor with 2000 tubes. This production rate of 0.12 t C_{5+} per single tube per day is in the range given in the literature for industrial FT fixed bed reactors (0.09 t C_{5+} per tube per day for cobalt and 0.07 t C_{5+} per tube and per day) for iron [40].
[2]Although compared to an iron catalyst, the diameter of the single tubes may be slighly smaller in the case of cobalt (about 25 % according to the data given in [40]), the tube diameter was kept constant for the simulation for a better comparison.

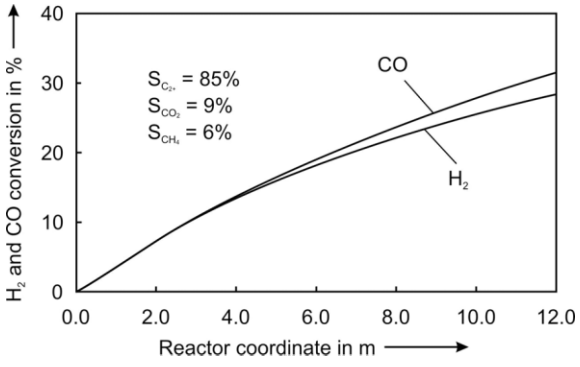

Figure 4. Profiles of H_2 and CO-conversion in the multi-tubular FT reactor (iron catalyst; tube diameter = 4.6 cm, $T_{in} = T_{cool}$ = 224 °C, T_{max} = 250 °C, two-dimensional model, parameters – see Tab. 1, axial temperature profile – see Fig. 7 below).

The fourth boundary condition is related to the heat transfer from the external tube side to the heat transfer medium (here, boiling water at about 25 bar):

$$\dot{q} = \alpha_{w,int}\left(T_{W,int,1} - T_{w,int,2}\right) = U_{wall}\left(T_{w,int,2} - T_{cool}\right) \quad \left(\text{with } U_{wall} = \left(\frac{d_{wall}}{\lambda_{wall}} + \frac{1}{\alpha_{W,ex}}\right)^{-1}\right) \tag{26}$$

U_{wall} summarizes the (small) thermal resistance of heat conduction by the wall (with thickness d_{wall}) and the heat transfer from the tube to the cooling medium, i.e., to the boiling water phase.

4.2 One-Dimensional Fixed Bed Reactor Model

It may be convenient to use a one-dimensional model (for details see [9]), where only axial gradients of temperature and concentration are considered. Like the two-dimensional model, this model also takes into account λ_{rad}, $\alpha_{w,int}$, λ_{wall}, and $\alpha_{w,ex}$, but now we assume a constant bed temperature and an overall thermal transmittance, $U_{overall}$, that lumps the conduc-

tion in the bed, heat transfer at and through the wall, and to the cooling medium by:

$$U_{\text{overall}} = \left(\frac{d_R}{8\lambda_{\text{rad}}} + \frac{1}{\alpha_{W,\text{int}}} + \frac{d_{\text{wall}}}{\lambda_{\text{wall}}} + \frac{1}{\alpha_{W,\text{ex}}} \right)^{-1} \quad (27)$$

whereby the difference of $d_{R,ex}$ and $d_{R,int}$ is neglected and, thus, we subsequently simply use $d_R \approx d_{R,int}$. Based on Eq. (27), the heat balance of the one-dimensional model is given by:

$$\rho_{\text{mol}} c_p u_s \frac{dT}{dz} = \frac{U_{\text{overall}} 4(T - T_{\text{cool}})}{d_R} - \rho_b \sum \Delta_R H_i r_{m,H_2,i} \quad (28)$$

5 Simulation Results

5.1 Results with Iron Catalyst

The results presented below by Figs. 4 to 8 were calculated using the commercial program, Presto-Kinetics (www.citwulkow.de). The maximum temperature is about 260 °C as the Fe-catalyst then starts to deactivate by sintering, which substantially lowers the internal surface area [22]. Hence, 250 °C was chosen as the maximum allowable temperature.

For an internal tube diameter of 46 mm (typically used in industrial fixed bed reactors) and a maximum temperature of 250 °C, we get a CO-conversion per pass of 32 % (see Fig. 4) and, thus, the total conversion with regard to the feed of 80 %, which is in good agreement with data given in the literature (conversion of 73 % [31]).

The selectivity to methane (6 % based on carbon) is also in agreement with data from the literature (5 % according to [45]). The conversion of hydrogen (28 %) is slightly lower than that of CO, which reflects the influence of the shift reaction which consumes CO, and forms H_2 and unwanted CO_2.

The influence of the cooling temperature on the axial temperature profiles in the multi-tubular FT reactor is shown in Fig. 5. We see that for a cooling temperature of more than about 245 °C, the reactor is very sensitive and a temperature runaway becomes likely.

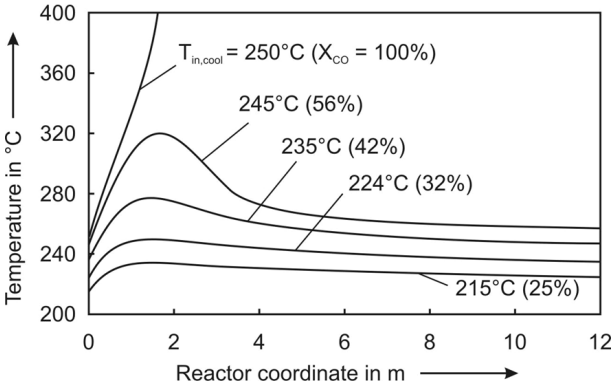

Figure 5. Influence of cooling temperature on the axial temperature profiles (iron catalyst: 4.6 cm in tube diameter, $T_{in} = T_{cool}$, two-dimensional reactor model, parameters – see Tab. 1).

In Fig. 6, the axial temperature profiles of the two- and one-dimensional model are compared for a cooling temperature of 224 °C. For the two-dimensional model, two profiles are given, the temperature exactly in the tube center and at the radial position 0.35 d_R.

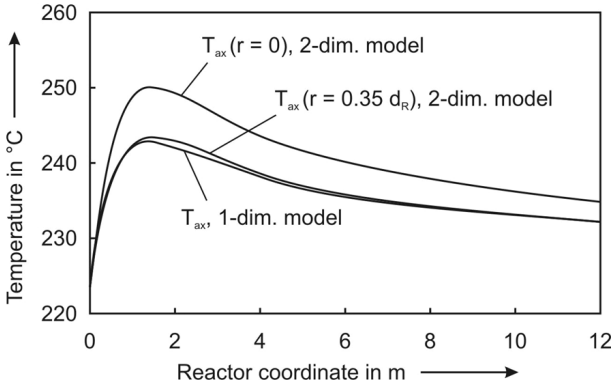

Figure 6. Axial temperature profiles in the multi-tubular FT reactor: comparison of the two- and one-dimensional models (Fe-catalyst: tube diameter = 4.6 cm, $T_{in} = T_{cool}$ = 224 °C, parameters in Tab. 1).

Fig. 6 indicates that the axial mean bed temperature profile of the one-dimensional model almost exactly equals the profile of the two-dimensional model at $r = 0.35\ d_R$.

This is in agreement with the theory [9]. As for the mean temperature of the one-dimensional model, this radial position is appropiate to divide the bed in the radial direction into two parts with equal volume. The good agreement of both models is underlined by the almost equal values of conversion (31.4 % for the one-dimensional and 31.5 % for two-dimensional).

The radial profiles at a distance from the reactor entrance of z = 1.5 m are shown in Fig. 7, both for the two- and one-dimensional model. At this axial position, we have the maximum axial temperature (see Fig. 5) and the most pronounced radial gradients in temperature.

The runaway behavior is shown in Fig. 8 by the plot of the axial maximum temperature versus the cooling temperature.

The two-dimensional model leads to a critical cooling temperature of 247 °C, whereas the one-dimensional model leads to 255 °C. Hence, if all heat transfer data are available, the more accurate two-dimensional model should be preferred.

5.2 Simulation Results with Cobalt Catalyst

As shown in Fig. 2, cobalt is more active than iron at temperatures above 210 °C. In addition, the rate is not inhibited by steam that is formed by the FT reaction. Hence, a lower temperature can be used to reach the same conversion (per pass), and to ensure a safe operation of the reactor. Fig. 9 (left) shows axial temperature profiles for different cooling temperatures.

For T_{cool} = 210 °C, the conversion (per pass) is 32 % and, for a recycle ratio of 2, almost complete conversion (96 %)

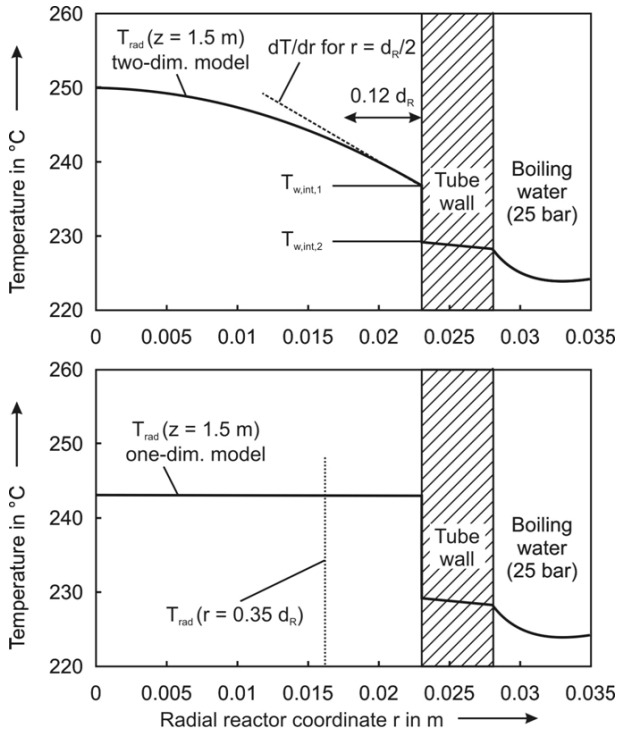

Figure 7. Radial temperature profiles in the single tube: comparison of the two-dimensional (above) and one-dimensional model (below). Iron catalyst, $T_{in} = T_{cool} = 224\,°C$, 1.5 m distance from the inlet).

could be achieved. A higher cooling temperature should not be used since, for the given tube diameter of 4.6 cm, a temperature runaway would be likely (see Fig. 9, right).

Figs. 9 and 5 indicate that the reaction temperatures are about 20 °C lower for cobalt ($T_{cool} = 210\,°C$, $T_{max} = 232\,°C$) compared to iron ($T_{cool} = 224\,°C$, $T_{max} = 250\,°C$) to reach the same conversion (here, 32 % per pass). Higher temperatures should be avoided to ensure a safe operation of the reactor, but also with regard to selectivity. According to [1, 29], the selectivity to methane and the yields of gasoline, diesel oil, and wax for cobalt are comparable to those for iron if the temperature of the Co-catalyst is 20 °C lower compared to Fe, e.g., the probability of chain growth is 0.92 for Co at 220 °C and 0.95 for Fe at 240 °C [29]. For $T > 250\,°C$ (Fe) and 230 °C (Co), too much unwanted methane is formed.

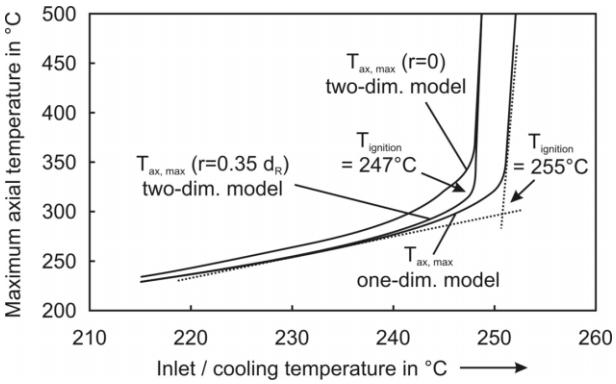

Figure 8. Influence of T_{cool} on the maximum axial temperature in the multi-tubular reactor (Fe-catalyst): comparison of the two- and one-dimensional model, $T_{in} = T_{cool}$, parameters – see Tab. 1).

6 Syngas Recycle and Overall Syngas Conversion

A flow sheet of a fixed bed reactor with recycle of syngas is shown in Fig. 10. For simplification of the subsequent calculations, we assume that the recycle gas only consists of unconverted CO and H_2. In reality, it also contains gases like methane and a purge stream is needed.

The unconverted syngas is returned to the reactor entrance after the separation of the products (here liquid hydrocarbons and water). Hence, the concentration of CO and H_2 remain unchanged (for the given simplified example). The recycle ratio, R, is defined as:

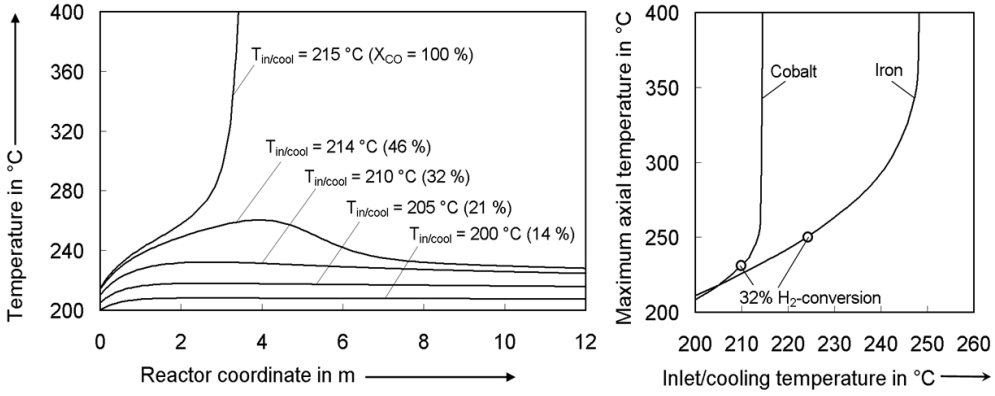

Figure 9. Influence of the cooling temperature on the axial temperature profiles for a cobalt catalyst (left) and on the maximum axial temperature in multi-tubular FT reactors for a cobalt and iron catalyst (right) (4.6-cm tube, $T_{in} = T_{cool}$, two-dimensional model, parameters – see Tab. 1).

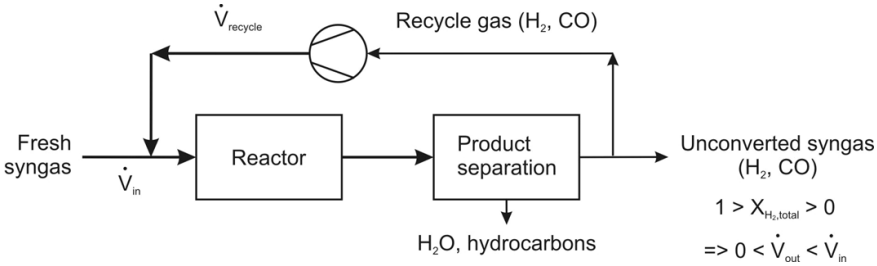

Figure 10. Simplified flow sheet of a FT fixed bed reactor with recycle of unconverted syngas.

$$R = \frac{\dot{V}_{\text{recycle}}}{\dot{V}_{\text{in}}} \tag{29}$$

If we consider plug flow behavior, a first-order reaction with respect to hydrogen and the use of the simplification of a constant volume reaction, the conversion of H_2 per pass is given by

$$X_{\text{H}_2,\text{per pass}} = 1 - e^{-k_{\text{m,H}_2,\text{eff}}\,\tau_{\text{per pass}}}$$

$$(\text{with} \quad \tau_{\text{per pass}} = \frac{m_{\text{cat}}}{\dot{V}_{\text{in}}(1+R)} = \frac{\tau}{(1+R)} \tag{30}$$

For the total conversion of hydrogen related to the hydrogen in the fresh feed, we have:

$$X_{\text{H}_2,\text{total}} = X_{\text{H}_2,\text{per pass}}(1+R) \tag{31}$$

and, hence, for $R = 1$, a conversion per pass of 50 % is needed for complete conversion. Eq. (31), i.e., $\dot{n}_{\text{H}_2,\text{recycle}}/\dot{n}_{\text{H}_2,\text{in}} = R$, is only valid if no inerts are in the recycle and if X_{CO} equals X_{H2}, and, thus, if the H_2-content in the recycle equals the content in the feed.

Insertion of Eq. (30) into Eq. (31) and substitution of the residence time per pass by the residence time related to the fresh feed leads to:

$$X_{\text{H}_2,\text{total}} = (1+R)\left(1 - e^{-\frac{k_{\text{m,H}_2}\tau}{(1+R)}}\right) = (1+R)\left(1 - e^{-\frac{\text{Da}}{(1+R)}}\right)$$
$$(\text{with } \tau = \frac{m_{\text{cat}}}{\dot{V}_{\text{in}}}) \tag{32}$$

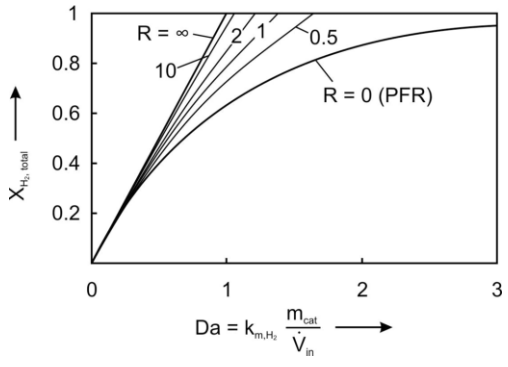

Figure 11. Influence of the recycle ratio on the total H_2-conversion (for conditions, see text).

Fig. 11 shows that for a given Damkoehler number, Da (defined based on the residence time related to the fresh feed), the total hydrogen conversion increases with the recycle ratio, *R*.

One final aspect should also be discussed: Syngas not only consists of CO and H_2, inerts such as CH_4 may be present. In addition, CO_2 (in the case of an iron catalyst) and CH_4 are formed (Eqs. (2) and (3)). Thus, even if CO_2 is completely removed from the off-gas before recycling, CH_4 will be present in the recycle and a purge gas stream is needed to avoid accumulation.

Figs. 12 and 13 show the respective mass balance for an iron catalyst (with water gas shift activity), a recycle ratio of 2.5, selectivities (based on carbon in CO) of 86 % for C_{2+}-hydrocarbons, 6 % for CH_4, 8 % for CO_2, and a composition of the fresh syngas of 64 % H_2, 32 % CO, and 4 % CH_4. The conversion is then lower than for the ideal case with no inerts in the

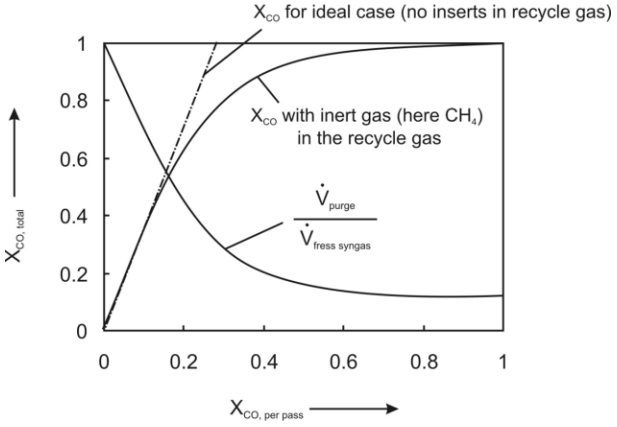

Figure 12. Influence of CO-conversion per pass on total conversion and purge gas stream for a recycle ratio of 2.5 (Fe-catalyst; selectivities based on C in CO: 86 % to C_{2+}-hydrocarbons, 6 % to CH_4, 8 % to CO_2; composition of fresh syngas: 64 % H_2, 32 % CO, and 4 % CH_4).

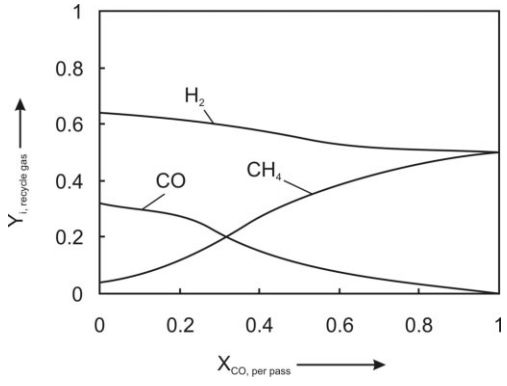

Figure 13. Composition of recycle gas for different values of CO-conversion per pass.

recycle. Fig. 12 also shows the amount of gas that has to be purged.

7 Room for Improvement of Fixed Bed FT Reactors by Enhanced Heat Transfer

There is still room for improvement in fixed bed FT reactors, e.g., by more active catalysts or by an enhanced heat transfer. The latter aspect was simulated by a stepwise disregard of the heat transfer resistances that determine the radial heat transfer from the fixed bed to the cooling medium (boiling water); see Tab. 2. At first, an infinite high value of the effective radial thermal conductivity, λ_{rad}, was assumed (case II). Then, in addition, the heat transfer coefficient, $\alpha_{W,int}$, was assumed to be infinitely high (case III), and, finally, the heat transfer coefficient of the external wall to boiling water, $\alpha_{W,ex}$, was also assumed to be infinitely high (which is unrealistic, but represents the ideal border case of an isothermal fixed bed). For the simulations, all (other) parameters were used as listed in Tab. 1 and the maximum temperature (= T_{in}) was kept constant (232 °C).

Tab. 2 indicates for the example of a cobalt catalyst that for the border case of an infinitely large effective radial thermal conductivity (λ_{rad}), the conversion would increase from 32 % (base case discussed in Section 5.2) to 40 %. If, in addition, the heat transfer resistance of the bed to the internal wall would also be negligible (infinite value of $\alpha_{W,int}$), the conversion would further increase to 42 %. Case III (infinitely large heat transfer coefficient of the external wall to boiling water, $\alpha_{W,ex}$) is also listed in Tab. 2 to show the theoretical optimum of an isothermal fixed bed without radial and axial temperature gradients (conversion of 44 %).

Although the results shown in Tab. 2 are "only" the result of simulations, the radial heat transfer parameters (λ_{rad} and $\alpha_{W,int}$) can really be improved, e.g., by a recycle of liquid hydrocarbons, as this increases the heat transfer in a packed bed for a cocurrent downflow of a gas and a liquid compared to pure gas flow, as shown in [46, 47]. This aspect is also discussed by Güttel, Kunz, and Turek [48], who proposed the use of structured packings (e.g., ceramic sponges) to improve the radial heat transfer (see also [49, 50]). The use of microstructured reactors for improvement of heat transfer is also an interesting option that should finally be mentioned [8, 39].

8 Conclusions

A two-dimensional pseudo-homogeneous reactor model was developed to simulate multi-tubular FT reactors. The model was used to simulate technical reactors for both iron and cobalt catalysts. The intraparticle diffusion limitations were taken into account by the effectiveness factor of pore diffusion. The model covers all the main aspects, i.e., the intrinsic kinetics of commercial Fe- and Co-catalysts, internal mass transfer, and all radial heat transfer parameters.

The main results of this study are:

- The comparison of the two-dimensional model with a simpler one-dimensional model shows that the CO-conversion is almost identical. To the contrary, the runaway behavior predicted by the one-dimensional model leads to a higher critical cooling temperature ($T_{ignition}$). For the iron catalyst and the chosen reaction conditions, $T_{ignition}$ is 255 °C compared to 247 °C of the two-dimensional model. Hence, if all heat transfer data are available, the more accurate two-dimensional model should be preferred.
- The effective reaction rate with cobalt is higher than with iron. Hence, a lower temperature can be used for Co. The calculations indicate that the temperatures in the reactor are about 20 °C lower for cobalt (T_{cool} = 210 °C, T_{max} = 232 °C) compared to iron (T_{cool} = 224 °C, T_{max} = 250 °C) to reach the same H_2-conversion (here 32 % per pass, i.e., almost complete conversion for a recycle ratio of 2). Higher temperatures should be avoided to ensure a safe operation of the reactor, but also with regard to product selectivity as the yields of methane, gasoline, diesel oil, and wax are then almost the same for cobalt and for iron.
- All results of the simulations are consistent with data given in the literature for fixed bed FT reactors based on cobalt and iron.
- There is still room for improvement of fixed bed FT reactors, e.g., by an enhanced heat transfer. For a cobalt catalyst, the conversion could be increased (theoretically) from 32 % (standard case) to 42 % if the heat transfer resistances of the radial heat conduction in the bed and of the heat transfer from the bed to the internal wall could be strongly decreased.

Table 2. Improvement of fixed bed FT reactors by enhanced heat transfer (Co-catalyst, all parameters – exept those given – as in Tab. 1, T_{max} = const. = 232 °C).

Case	CO-conversion [%]	T_{cool} (= T_{in}) [°C]
I) Base case (see Section 5.2)	32.1	210
II) Base case with infinitely large effective radial thermal conductivity, λ_{rad}	40.0	219
III) Case II, but also with an infinitely large heat transfer coefficient bed to internal wall, $\alpha_{W,int}$	42.3	227
IV) Case III, but also with an infinitely large heat transfer coefficient of external wall to boiling water, $\alpha_{W,ex}$	43.8	232

Symbols used

ARGE		Arbeitsgemeinschaft (consortium) Ruhrchemie/Lurgi
$A_{p,ex}$	[m^2]	external surface area of a catalyst particle
c	[mol/m^3]	concentration
c_p	[J/(mol K)]	heat capacity of the gas phase
d_p	[m]	diameter of a particle
$d_{R,int}$	[m]	internal diameter of a single tube
$d_{R,ex}$	[m]	external diameter of a single tube
Da	[–]	Damkoehler number (= $k_m \tau$)
D_{eff}	[m^2/s]	effective dispersion coefficient
D_{mol}	[m^2/s]	molecular diffusion coefficient
E_A	[J/mol]	activation energy
$H_{H2,c}$	[Pa m^3/mol)	Henry coefficient
$k_{m,HW}$	[m^3/(kg s)]	rate constant for the Hougen-Watson equation for iron
k_m	[m^3/(kg s)]	rate constant for the (pseudo-) first order equation
$k_{m,LH}$	[m^6/(mol kg s)]	rate constant for the Langmuir-Hinshelwood equation for FT on Co (Eq. (15))
$k_{m,eff}$	[m^3/(kg s)]	effective reaction rate constant
K_{HW}	[–]	coefficient in the Hougen-Watson rate equation for FT on Fe (Eq. (4))
K_{CO}	[m^3/mol]	adsorption coefficient for CO
m_{cat}	[kg]	mass of the catalyst
$\dot{n}$	[mol/s]	molar flow rate
r_m	[mol/(kg s)]	reaction rate per unit of mass of the catalyst
$r_{m,eff}$	[mol/(kg s)]	effective rate per mass of the catalyst
p	[Pa]	total pressure
p_i	[Pa]	partial pressure of component i
$\dot{q}$	[W(m^2]	heat flux
r	[m]	radial direction
R	[J/(mol K)]	ideal gas law constant
R	[–]	recycle rate
T	[°C, K]	temperature
u_s	[m/s]	superficial gas velocity
$U_{overall}$	[W/(m^2K)]	overall thermal transmittance
U_{wall}	[W/(m^2K)]	thermal transmittance
V_p	[m^3]	particle volume
$\dot{V}$	[m^3/s]	volume flow rate
X	[–]	conversion

Greek symbols

$\alpha_{W,int}$	[W/m^2 K)]	heat transfer coefficient from the bed to the internal wall
$\alpha_{W,ex}$	[W/m^2 K)]	heat transfer coefficient from the outer shell of the tube to boiling water
$\Delta_R H^0_{298}$	[J/mol]	heat of reaction (at 1 bar, 298 K)
ε_P	[–]	porosity of a particle
ϕ	[–]	Thiele modulus
η_{pore}	[–]	pore effectiveness factor
λ_{rad}	[W/(m K)]	effective radial heat conduction in the fixed bed
λ_{wall}	[W/(m K)]	thermal conductivity of the reactor wall material
ρ_P	[kg/m^3]	density of the catalyst
ρ_b	[kg/m^3]	bulk density of the catalyst bed
ρ_{mol}	[mol/m^3]	molar density of the gas phase
τ_P	[–]	particle tortuosity
t	[kg s/m^3]	modified residence time

Subscripts

in	reactor inlet
cool	cooling
g	gas phase
l	liquid
S	related to (water gas) shift reaction
M	related to methane formation

References

[1] A. Steynberg, M. Dry, M. E. Davis, B. B. Breman, in *Fischer-Tropsch Technology, Studies in Surface Science and Catalysis 152*, (Eds: A. Steynberg, M. Dry), Elsevier, Amsterdam **2004**.

[2] H. E. Atwood, C. O. Bennett, *Ind. Eng. Chem. Process. Des. Dev.* **1979**, *18*, 163.

[3] G. Bub, M. Baerns, *Chem. Eng. Sci.* **1980**, *35*, 348.

[4] A. Jess, R. Popp, K. Hedden, *Appl. Cat. A. Gen.* **1999**, *186*, 321.

[5] Y. N. Wang et al., *Chem. Eng. Sci.* **2003**, *58*, 867.

[6] J. W. A. De Swart, *Ph.D. Thesis*, University of Amsterdam, Netherlands, **1996**.

[7] J. W. A. De Swart, R. Krishna, S. T. Sie, in *Natural gas conversion IV, Studies in Surface Science and Catalysis 107*, (Eds: M. de Pontes, R. L. Espinoza, C. P. Nicolaides, J. H. Scholz, M. S. Scurrell), Elsevier, Amsterdam **1997**.

[8] R. Güttel, T. Turek, *Chem. Eng. Sci.* **2009**, *64*, 955.

[9] G. F. Froment, K. B. Bischoff, *Chemical Reactor Analysis and Design*, Wiley, New York **1990**.

[10] G. A. Huff, C. N. Satterfield, *Ind. Eng. Chem. Proc. Des. Dev.* **1984a**, *23*, 696.

[11] I. C. Yates, C. N. Satterfield, *Energy & Fuels* **1991**, *5*, 158.

[12] T. J. Donnelly, C. N. Satterfield, *Appl. Cat. A Gen.* **1989**, *52*, 93.

[13] M. E. Dry, *J. of Molecular Cat.* **1982**, *17*, 133.

[14] F. A. N. Fernandes, *Chem. Eng. Technol.* **2005**, *28*, 930.

[15] G. A. Huff, C. N. Satterfield, *J. of Catalysis* **1984b**, *85*, 370.

[16] M. F. M. Post, J. K. Van't Hoog, J. K. Minderhoud, S. T. Sie, *AIChE J.* **1989**, *35*, 1107.

[17] T. Riedel et al., *Appl. Cat. A General* **1999**, *186*, 201.

[18] H. Schulz, M. Claeys, *Appl. Cat. A General* **1999**, *186*, 91.

[19] H. Schulz, G. Schaub, M. Claeys, T. Riedel, *Appl. Cat. A Gen.* **1999**, *186*, 215.

[20] E. Van Steen, H. Schulz, *Appl. Cat. A Gen.* **1999**, *186*, 309.

[21] E. Van Steen, *Ph.D. Thesis*, University Karlsruhe, Germany **1993**.

[22] T. Kuntze, *Ph.D. Thesis*, University Karlsruhe, Germany **1991**.

[23] H. Raak, *Ph.D. Thesis*, University Karlsruhe, Germany **1995**.

[24] C. R. Wilke, P. Chang, *AICHE J.* **1986**, *1*, 264.
[25] R. Popp, *Ph.D. Thesis*, University Karlsruhe, Germany **1996**.
[26] C. Maretto, R. Krishna, *R. Cat. Today* **1999**, *52*, 279.
[27] R. B. Anderson, *The Fischer-Tropsch Synthesis*, Academic Press, Orlando **1984**.
[28] M. E. Dry, *Catal. Sci. Technol.* **1981**, *1*, 159.
[29] M. E. Dry, *Catalysis Today* **2002**, *71*, 227.
[30] J. Eilers, S. A. Postuma, S. T. Sie, *Catalysis Letters* **1990**, *7*, 253.
[31] *Chemierohstoffe aus Kohle* (Ed: J. Falbe), Georg Thieme Verlag, Stuttgart, Germany **1977**.
[32] M. W. Haenel, *Erdoel Erdgas Kohle* **2006**, *122*, 78.
[33] H. Schulz, *Appl. Cat. A General* **1999**, *186*, 3.
[34] R. Zennaro, F. Hugues, E. Caprani, *DGMK/SCI Conference: Synthesis Gas Chemistry*, Dresden, Germany, October **2006**.
[35] G. Schaub, R. Rohde, A. M. Subiranas, DGMK/*SCI Conference: Synthesis Gas Chemistry*, Dresden, Germany, October **2006**.
[36] S. T. Sie, R. Krishna, *Fuel Proc. Tech.* **2000**, *64*, 73.
[37] S. T. Sie, R. Krishna, *Appl. Cat. A General* **1999**, *186*, 55.
[38] S. T. Sie, M. M. G. Senden, H. M. H. Van Wechem, *Cat. Today* **1991**, *8*, 371.
[39] R. Güttel, U. Kunz, T. Turek, *Chem. Eng. Tech.* **2008**, *31*, 746.
[40] J. R. Farrauto, C. H. Bartholomew, *Fundamentals of industrial catalytic processes*, 2nd ed., Wiley, New York **2006**.
[41] *VDI-Wärmeatlas: Berechnungsblätter für den Wärmeübergang*, 9th ed., Springer-Verlag, Berlin, Heidelberg **2002**.
[42] M. Nilles, *Ph.D. Thesis*, University of Karlsruhe, Germany **1991**.
[43] E.-U. Schlünder, *Einführung in die Wärmeübertragung*, Vieweg & Sohn, Braunschweig, Wiesbaden, Germany **1986**.
[44] E.-U. E. Schlünder, E. Tsotsas, *Wärmeübertragung in Festbetten, durchmischten Schüttgütern und Wirbelschichten*, Georg Thieme Verlag, Stuttgart, Germany **1988**.
[45] H. G. Franck, A. Knop, *Kohleveredlung*, Springer, Berlin, Heidelberg **1979**.
[46] A. S. Mamine, L. Gerth, H. De Gall, G. Wild, *Chem. Eng. Sci.* **1996**, *51*, 3813.
[47] N. J. Mariani, O. M. Martinez, G. F. Barreto, *Chem. Eng. Sci.* **2001**, *56*, 5995.
[48] R. Güttel, U. Kunz, T. Turek, *Chem. Ing. Tech.* **2007**, *79*, 531.
[49] M. V. Twigg, J. T. Richardson, *Chem. Eng. Res. & Design* **2002**, *80*, 183.
[50] A. Reitzmann, F. C. Patcas, B. Kraushaar-Czarnetzki, *Chem. Ing. Tech.* **2006**, *78 (7)*, 885. DOI: 10.1002/cite.200600029.

